International Journal of Science and Engineering (IJSE)

Home page: http://ejournal.undip.ac.id/index.php/ijse

Dual solutions for MHD stagnation-point flow of a nanofluid over a stretching surface with induced magnetic field

Sandeep Naramgari[1], C. Sulochana[2#]

[1, 2#] Department of Mathematics, Gulbarga University, Gulbarga-585106, India.
Email: math.sulochana@gmail.com

Abstract *- Present study deals with the buoyancy-driven MHD mixed convection stagnation-point flow, heat and mass transfer of a nanofluid over a non-isothermal stretching sheet in presence of induced magneticfield, radiation, chemical reaction, suction/injection and heat source/sink. The basic governing partial differential equations are reduced to a set of ordinary differential equations by using appropriate similarity transformation. The resulting system is solved numerically by bvp5c Matlab package. Numerical results are validated by comparing with the published results. The influence of non-dimensional governing parameters on velocity, induced magneticfield, temperature and concentration profiles along with coefficient of skin friction, local Nusselt and Sherwood numbers are discussed and presented with the help of graphs and tables. Comparisons are made with the existed studies. Results indicate that dual solutions exists only for certain range of suction/ injection parameter and injection parameter have tendency to enhance the momentum, thermal and concentration boundary layer thickness.*

Keywords— *Stagnation-point flow, Mixed convection, Nanofluid, Induced magneticfield Radiation, Chemical Reaction..*

Submission: May 10, 2015 Corrected : June 8, 2015 Accepted: June 30, 2015
Doi: 10.12777/ijse.9.1.1-8

*[**How to cite this article**:* Naramgari, S. and C. Sulochana*. (2015).* Dual solutions for MHD stagnation-point flow of a nanofluid over a stretching surface with induced magneticfield *International Journal of Science and Engineering, 9(1),1-8.* **Doi**: 10.12777/ijse.9.1.1-8*]*

I. INTRODUCTION

Many Stagnation point flow, heat and mass transfer over stretching sheet have variety of applications like transpiration, wire drawing, hot rolling, paper production, oil recovery etc. The study of MHD flow over a stretching sheet has various applications in modern metallurgy and metal-working processes. In view of these applications (Massoudi and Ramezan, 1990) started the revolution of stagnation point flow by analyzing the heat transfer characteristics of boundary layer flow of a viscoelastic fluid towards stagnation point. (Ali *et al.*, 2011) discussed the MHD stagnation-point flow and heat transfer towards stretching sheet in presence of induced magneticfield. (Sulochana and Sandeep, 2015) studied the stagnation-point flow and heat transfer of Cu-water nanofluid towards horizontal and exponentially stretching or shrinking cylinders. Radiation and viscous dissipation effects on stagnation-point flow of a micropolar fluid over a stretching surface in presence of suction and injection effects was studied by (Jayachandra Babu *et al.*, 2015). (Makinde *et al.*, 2013) discussed stagnation point flow and heat transfer of a nanofluid past a convectively heated stretching or shrinking sheet by considering buoyancy effects. Flow and heat transfer at a stagnation point flow over an exponentially vertical shrinking sheet with suction effect was illustrated by (Rohni *et al.*, 2014). (Akbar *et al.*, 2015) analyzed the effects of induced magneticfield and heat flux of carbon nano tubes for peristaltic flow in a permeable channel. (Sandeep and Sulochana, 2015) presented dual solutions for MHD nanofluid flow over an exponentially stretching sheet by considering heat generation/absorption and radiation. (Sandeep *et al.*, 2013) discussed the radiation effect on an unsteady natural convective flow of a nanofluid past an infinite vertical plate. (Raju *et al.*, 2015) studied the heat and mass transfer of MHD fluid over a flat plate and stretching surface.

Radiation and magneticfield effects on unsteady natural convection flow of a nanofluid past an infinite vertical plate in presence of heat source was studied by (Mohankrishna *et al.*, 2014). (Rashidi *et al.*, 2014) analyzed the MHD free convective heat and mass over a permeable vertical stretching sheet in the presence of radiation and buoyancy effects. (Makinde and Aziz, 2011) illustrated the boundary layer flow of a nanofluid over a stretching sheet in presence of convective boundary conditions. Radiation effects on the flow of Powell- Eyring fluid over an unsteady inclined stretching sheet with non-uniform heat source/sink was discussed by (Hayat *et al.*, 2014). The influence of thermal radiation on MHD nanofluid flow and heat transfer using two phase model was presented by (Sheikholeslami *et al.*, 2015). (Elbashbeshy, 2001) studied the heat transfer in a nanofluid over an exponentially stretching continuous surface with suction effect. (Subhashini *et al.*, 2014) presented dual solutions for mixed convection flow of a nanofluid near the stagnation point past an exponentially stretching/shrinking sheet.

Effect of partial slip on MHD flow over a porous stretching sheet with non-uniform heat source/sink and thermal radiation along with wall mass transfer was discussed by (Hakeem *et al.*, 2014). (Cortell, 2014) studied the MHD flow and radiative nonlinear heat transfer of a viscoelastic fluid over a stretching sheet with heat generation or absorption. (Bhattacharya, 2013) discussed the stagnation point flow of a Casson fluid towards a stretching or shrinking sheet. (Mustafa *et al.*, 2013) discussed boundary layer flow of a nanofluid over an exponentially stretching sheet with convective boundary conditions. Stagnation point flow and mass transfer past a stretching or shrinking cylinder in presence of chemical reaction was studied by (Najib *et al.*, 2014). Heat transfer characteristics of the flow over an exponentially porous stretching sheet with surface heat flux in porous medium were discussed by (Chandra Mandal and Swati, 2013). (Pal and Mandal, 2014) illustrated the effect of thermal radiation on mixed convection stagnation point flow over a stretching or shrinking sheet in porous medium. (Sandeep *et al.*, 2012) studied the radiation and chemical reaction effects on MHD free convective flow over a vertical plate. (Rana and Bhargava, 2012) presented a numerical study to analyze the flow and heat transfer of a nanofluid over a nonlinearly stretching sheet.

In this study we analyzed the buoyancy-driven MHD mixed convection stagnation-point flow, heat and mass transfer of a nanofluid over a non-isothermal stretching sheet in presence of induced magneticfield, radiation, chemical reaction, suction/injection and heat source/sink. The basic governing partial differential equations are reduced to a set of ordinary differential equations by using appropriate similarity transformation. The resulting system is solved numerically by bvp5c Matlab package. Numerical results are validated by comparing with the published results. The influence of non-dimensional governing parameters on velocity, induced magneticfield, temperature and concentration profiles along with coefficient of skin friction, local Nusselt and Sherwood numbers are discussed and presented with the help of graphs and tables.

II. MATHEMATICAL FORMULATION

Consider a steady, two-dimensional, viscous incompressible mixed convection electrically conducting stagnation point flow of a nanofluid over a stretching surface in the presence of induced magneticfield. The stretching sheet is considered along the $x-$axis and $y-$axis is normal to it. It is assumed that the sheet is non-conducting and the applied magneticfield of uniform strength H_0. It is also assumed that the induced magneticfield is applied in $y-$direction and the parallel component H_1 approaches the value $H_e = H_0$ in the free stream flow and normal component of the induced magneticfield H_2 vanishes near the wall. T_w and T_∞ are respectively indicates the temperatures near and far away from the wall and C_w and C_∞ are respectively indicates the concentration near and far away from the wall. $u_w = cx$ and $u_e = ax$ are the stretching and free stream velocities respectively, where a, c are positive constants. In addition with this radiation and chemical reaction effects are taken into account. The physical model and coordinate system is displayed in Fig.1

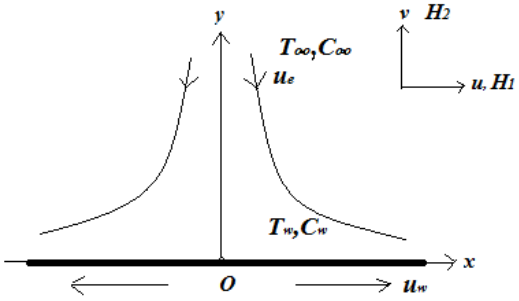

Fig.1 Physical model and coordinate system

Under the above assumptions the governing boundary layer equations are given by (Ali *et al.*, 2011)

$$\frac{\partial u}{\partial x}+\frac{\partial v}{\partial y}=0, \tag{1}$$

$$\frac{\partial H_1}{\partial x}+\frac{\partial H_2}{\partial y}=0, \tag{2}$$

$$\left.\begin{aligned} u\frac{\partial u}{\partial x}+v\frac{\partial v}{\partial y}=\frac{\mu_{nf}}{\rho_{nf}}\frac{\partial^2 u}{\partial y^2}-\frac{\mu_0}{4\pi\rho_{nf}}\left(H_1\frac{\partial H_1}{\partial x}+H_2\frac{\partial H_1}{\partial y}\right)- \\ \frac{\mu_0}{4\pi\rho_{nf}}H_e\frac{\partial H_e}{\partial x}+u_e(x)\frac{\partial u_e(x)}{\partial x} \\ +\frac{(\rho\beta)_{nf}}{\rho_{nf}}g(T-T_\infty)+\frac{(\rho\beta^*)_{nf}}{\rho_{nf}}g(C-C_\infty), \end{aligned}\right\} \tag{3}$$

$$u\frac{\partial H_1}{\partial x}+v\frac{\partial H_1}{\partial y}=H_1\frac{\partial u}{\partial x}+H_2\frac{\partial u}{\partial y}+\alpha_1\frac{\partial^2 H_1}{\partial y^2}, \tag{4}$$

$$u\frac{\partial T}{\partial x}+v\frac{\partial T}{\partial y}=\alpha_{nf}\frac{\partial^2 T}{\partial y^2}-\frac{1}{(\rho c_p)_{nf}}\frac{\partial q_r}{\partial y}-\frac{Q_0}{(\rho c_p)_{nf}}(T-T_\infty), \tag{5}$$

$$u\frac{\partial C}{\partial x}+v\frac{\partial C}{\partial y}=D_m\frac{\partial^2 C}{\partial y^2}-k_0(C-C_\infty), \tag{6}$$

With the boundary conditions

$$\left.\begin{aligned} &u=u_w(x), v=V_w, \frac{\partial H_1}{\partial y}=H_2=0, T=T_\infty+T_0(x/L), \\ &C=C_\infty+C_0(x/L) \text{ at } y=0, \\ &u=u_e(x), v\to 0, H_1=H_e(x)=H_0(x/L), \\ &T\to T_\infty, C\to C_\infty, \qquad \text{as } y\to\infty, \end{aligned}\right\} \tag{7}$$

where u, v velocity components in x, y directions, H_1, H_2 are the magnetic components in x, y directions, ρ_{nf} and μ_{nf} are the nanofluid density and dynamic viscosity respectively, β_{nf} is the thermal expansion of the nanofluid, g is the acceleration due to gravity, σ is the electrical conductivity, $(\rho c_p)_{nf}$ is the specific heat capacitance of nanofluid, T, C are the fluid temperature and concentration, T_0, C_0 are the reference temperature and concentration, k_{nf} is the effective thermal conductivity of nanofluid, α_{nf} is the thermal diffusivity of the nanofluid, $\alpha_1 = 1/4\pi\sigma$ is the magnetic diffusivity, μ_0 is the magnetic permeability, Q_0 is the heat source/sink parameter, D_m is the mass diffusivity,

k_0 is the chemical reaction and V_w is the suction/injection velocity. The radiative heat flux q_r under Rosseland approximation is the form

$$q_r = -\frac{4\sigma^*}{3k^*}\frac{\partial T^4}{\partial y}, \quad (8)$$

where σ^* is the Stefan-Boltzmann constant and k^* is the mean absorption coefficient. The temperature differences within the flow are assumed to be sufficiently small such that T^4 may be expressed as a linear function of temperature. Expanding T^4 using Taylor series and neglecting higher order terms yields

$$T^4 \cong 4T_\infty^{\ 3}T - 3T_\infty^{\ 4}, \quad (9)$$

To convert the governing equations in to set of nonlinear ordinary differential equations we now introducing the following similarity transformation

$$u = cxF'(\eta), v = -\sqrt{\nu_f c}F(\eta),$$
$$\eta = \sqrt{c/\nu_f}\,y, H_1 = H_0(x/L)G'(\eta),$$
$$H_2 = -(H_0/L)\nu_f^{1/2}c^{-1/2}G(\eta), \theta(\eta) = \frac{T-T_\infty}{T_w-T_\infty}, \psi(\eta) = \frac{C-C_\infty}{C_w-C_\infty}, \quad (10)$$

Substituting equations (8)-(10) in to (1)-(7), we get the following nonlinear coupled ordinary differential equations:

$$F''' + \left(\frac{a^2}{c^2} + FF'' - F'^2\right) + M\left(G' - GG'' - 1\right) + \Lambda\theta + \Gamma\psi = 0, \quad (11)$$

$$G''' - \mathrm{Pr}_m(F''G - FG'') = 0, \quad (12)$$

$$\frac{1}{\mathrm{Pr}}\left(1 + \frac{4}{3}R\right)\theta'' + F\theta' - F'\theta - Q_H\theta = 0, \quad (13)$$

$$\frac{1}{Sc}\psi'' + F\psi' - F'\psi - Kr\psi = 0, \quad (14)$$

with the transformed boundary conditions

$$\left.\begin{aligned} &F = S, F' = 1, G = G'' = 0, \theta = 1, \psi = 1, \text{ at } \eta = 0, \\ &F' = a/c, G' = 1, \theta = 0, \psi = 0, \quad \text{as } \eta \to \infty, \end{aligned}\right\} \quad (15)$$

where M is the magneticfield parameter, Λ, Γ are the buoyancy parameters, Pr is the Prandtl number, Pr_m is the magnetic Prandtl number, R is the radiation parameter, Q_H is the heat source/sink parameter, Sc is the Schmidt number, Kr is the chemical reaction parameter and S is the suction/injection parameter with $S > 0$ for suction and $S < 0$ for injection, which are given by

$$\left.\begin{aligned} &M = \frac{\mu_0 H_0^2}{4\pi\rho_f L^2 c^2}, \Lambda = \frac{g\beta_f(T_w-T_\infty)}{c^2 L} = \frac{Gr}{\mathrm{Re}^2}, \Gamma = \frac{g\beta_f^*(C_w-C_\infty)}{c^2 L} = \frac{Gc}{\mathrm{Re}^2}, \\ &Gr = \frac{g\beta_f(T_w-T_\infty)L^3}{\nu_f^2}, Gc = \frac{g\beta_f^*(C_w-C_\infty)L^3}{\nu_f^2}, \mathrm{Re}^2 = \frac{L^4c^2}{\nu_f^2}, \mathrm{Pr} = \frac{\nu_f}{\alpha_f}, \\ &\mathrm{Pr}_m = \frac{\nu_f}{\alpha_1}, R = \frac{4\sigma^* T_\infty^3}{k^* k_f}, Q_H = \frac{Q_0}{(\rho c_p)_f c} Sc = \frac{\nu_f}{D_m}, Kr = \frac{k_0}{c}, S = -\frac{V_w}{(\nu_f c)^{1/2}}, \end{aligned}\right\} \quad (16)$$

For engineering interest the shear stress coefficient or friction factor C_f and local Nusselt number Nu_x and Sherwood number Sh_x are given by

$$\mathrm{Re}_x^{1/2} C_f = \frac{1}{(1-\phi)^{2.5}} f''(0), \quad (17)$$

$$\mathrm{Re}_x^{-1/2} Nu_x = -\frac{k_{nf}}{k_f}\theta'(0), \quad (18)$$

$$\mathrm{Re}_x^{-1/2} Sh_x = -\psi'(0), \quad (19)$$

III. RESULTS AND DISCUSSION

The system of nonlinear ordinary differential equations (11) to (15) with the boundary conditions (16) are solved numerically by using bvp5c Matlab package. Results obtained shows the effects of the various non-dimensional governing parameters, namely magneticfield parameter (M), buoyancy parameter (Λ), radiation parameter (R), heat source/sink parameter (Q_H) and chemical reaction parameter (Kr) on the velocity, induced magneticfield and temperature profiles of the flow. Also, the friction factor and Nusselt number is discussed and presented in tabular form. For numerical results we considered $\mathrm{Pr}_m = a/c = M = \Lambda = \Gamma = 1, R = Q_H = Kr = 0.5, \mathrm{Pr} = 6.8$, and $Sc = 0.6$. These values are kept as common in entire study except the varied values as shown in respective figures and tables.

Figs. 2 and 3 show the influence of magneticfield parameter on velocity and induced magneticfield profiles for suction and injection cases. It is evident from the figures that an increase in magneticfield parameter enhances the velocity and induced magneticfield profiles for both suction and injection cases. Generally, in presence of induced magneticfield the external magneticfield acts like drag force and develops the body force, which causes to accelerate the flow and enhance the momentum boundary layers. Figs. 4-6 display the effect of radiation parameter on velocity, induced magneticfield and temperature profiles for suction and injection cases. It is clear that an enhancement in the radiation parameter increases the velocity, induced magneticfield and temperature profiles for suction and injection cases. Increase in radiation parameter releases the heat energy to the flow, which causes to develop the momentum and thermal boundary layer thicknesses.

Figs.7-9 represents the influence of heat source/sink parameter on velocity, induced magneticfield and temperature profiles for suction and injection cases. It is noticed from the figures that a raise in the value of heat source/sink parameter depreciates the velocity, induced magneticfield and temperature profiles for suction and injection cases. This concludes that the parameter Q_H acts like heat sink. Due to this reason we seen fall in the velocity and thermal boundary layer thicknesses. The influence of thermal buoyancy parameter on velocity and induced magneticfield profiles for suction and injection cases are displayed in Figs. 10 and 11. It is clear that an increase in thermal buoyancy parameter enhances the velocity and induced magneticfield profiles. This is due to the fact that the enhancement in thermal buoyancy parameter accelerates the flow and develops the momentum boundary layer thickness.

Figs.12-14 depicts the effect of chemical reaction parameter on velocity, induced magneticfield and temperature profiles for suction and injection cases. It is observed from the figures that a raise in the value of chemical reaction parameter depreciates the velocity, induced magneticfield and temperature profiles for suction and injection cases. The similar type of results is noticed form Figs. 15-17 as displayed for Schmidt number influence on velocity, induced magneticfield and temperature profiles for suction and injection cases. Physically, the increase in the Schmidt number causes to reduce in molecular diffusion. Hence, the concentration of the species is higher for lower values of Sc and lower for higher values of Sc.

Table 1 shows the comparison of the present results with the existed results. Present results have an excellent agreement with the existed results of (Ali *et al.*, 2011) under some special assumptions. This depicts the validity of the present study along with the accuracy of the numerical technique we used in this study. Table 2 displays the effect of non-dimensional governing parameters on friction factor, Nusselt and Sherwood numbers. It is evident from the table that an increase in magneticfield parameter and thermal buoyancy parameter enhances the friction factor along with heat and mass transfer rate. A raise in the values of chemical reaction parameter and Schmidt number depreciates the skin friction coefficient and Nusselt number but enhances the Sherwood number. An increase in radiation parameter increases the friction factor, mass transfer rate and declines the heat transfer rate. But heat source/sink parameter shows opposite results to the radiation parameter.

Table.1 Comparison of the values of $f''(0)$ when $M = \Lambda = \Gamma = R = Q_H = Sc = Kr = 0$.

a/c	Ali et al. (2011)	Present study
0.1	-0.9694	-0.9695
0.2	-0.9181	-0.9182
0.5	-0.6673	-0.6673
2.0	2.0175	2.0175
3.0	4.7293	4.7294

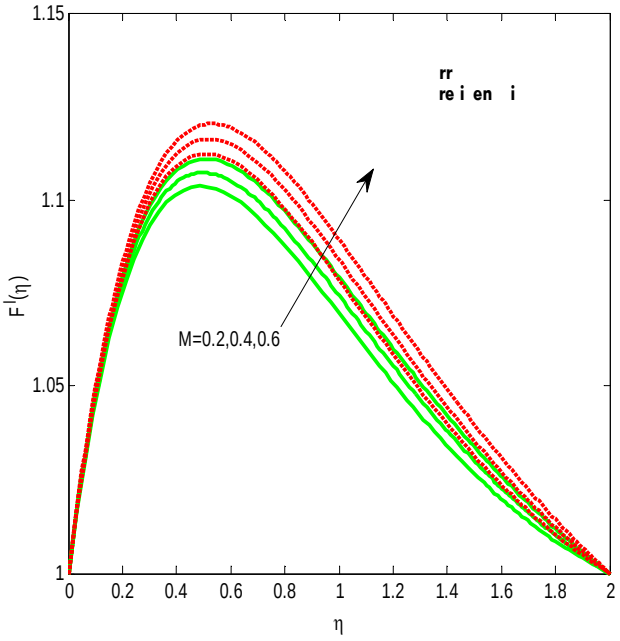

Figure 2. Velocity profiles for different values of magneticfield parameter

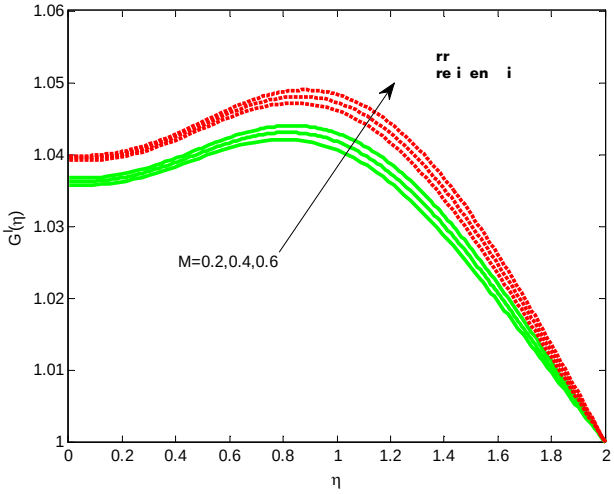

Figure 3. Induced magneticfield profiles for different values of magneticfield parameter

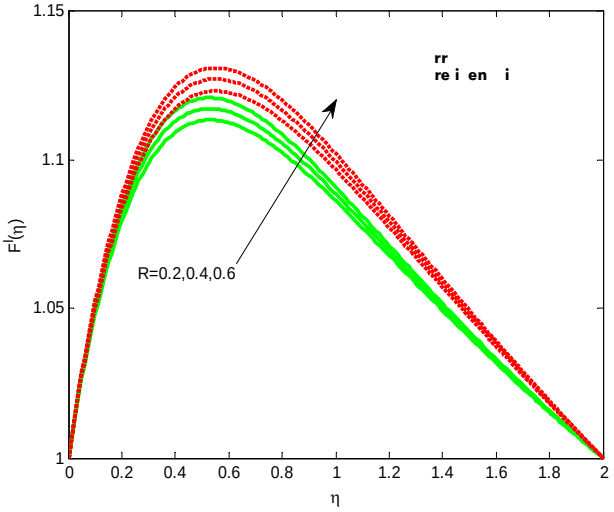

Figure 4. Velocity profiles for different values of radiation parameter

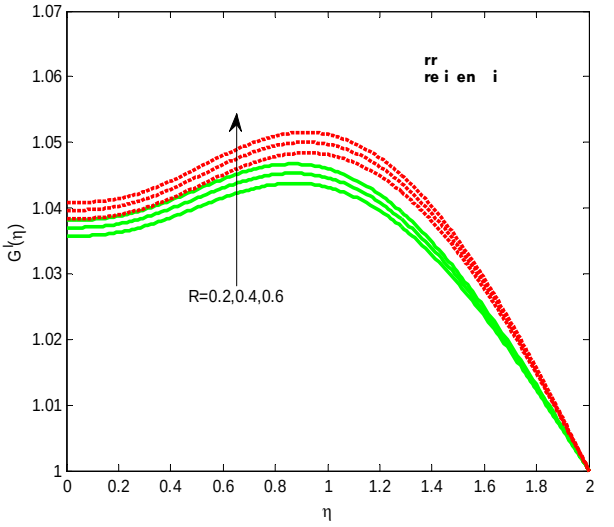

Figure 5. Induced magneticfield profiles for different values of radiation parameter

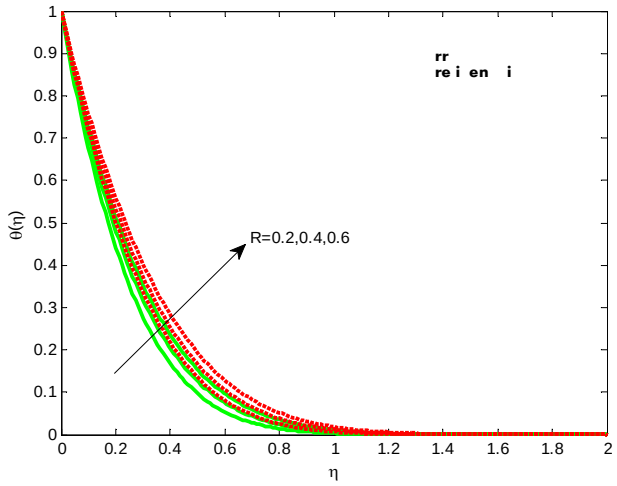

Figure 6. Temperature profiles for different values of radiation parameter

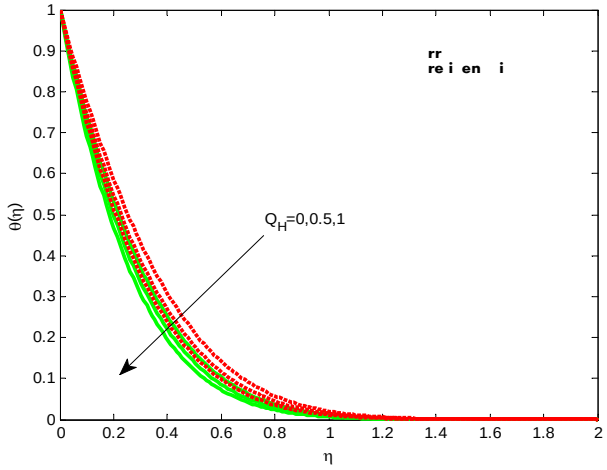

Figure 9. Temperature profiles for different values of heat source/sink parameter

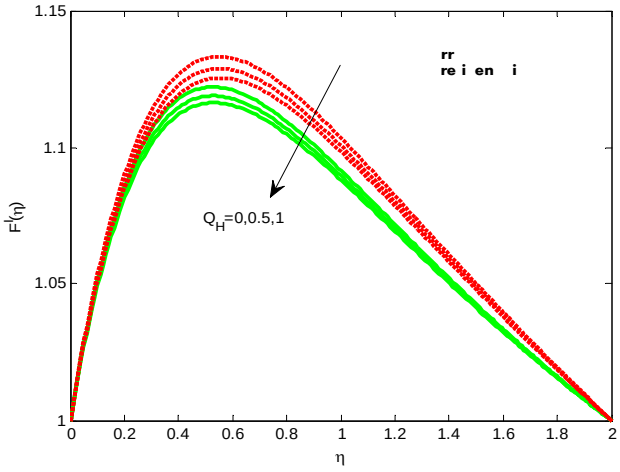

Figure 7. Velocity profiles for different values of heat source/sink parameter

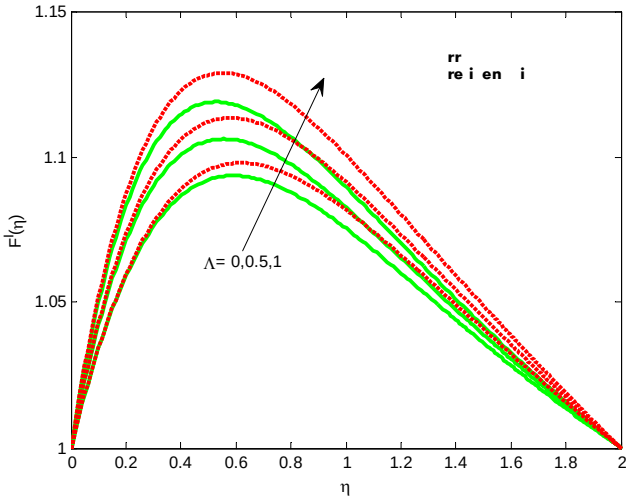

Figure 10. Velocity profiles for different values of thermal buoyancy parameter

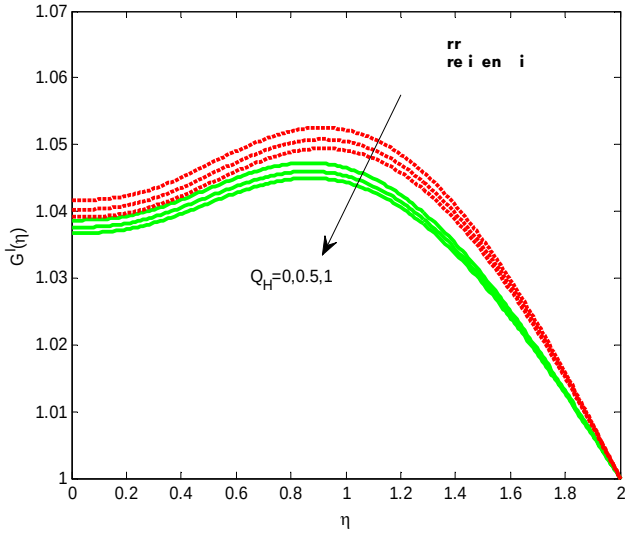

Figure 8. Induced magneticfield profiles for different values of heat source/sink parameter

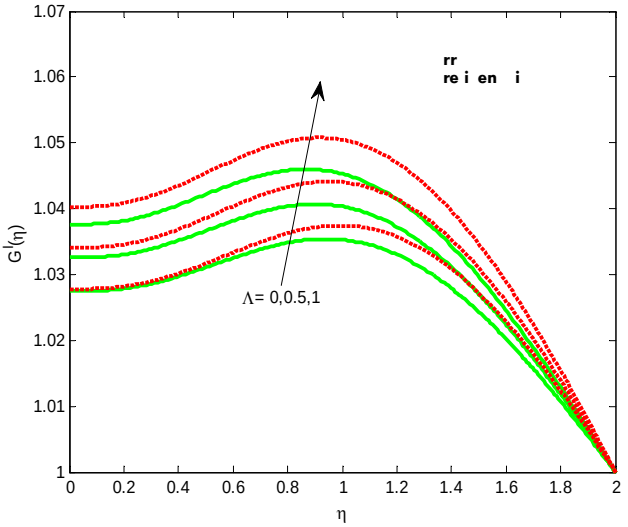

Figure 11. Induced magneticfield profiles for different values of thermal buoyancy parameter

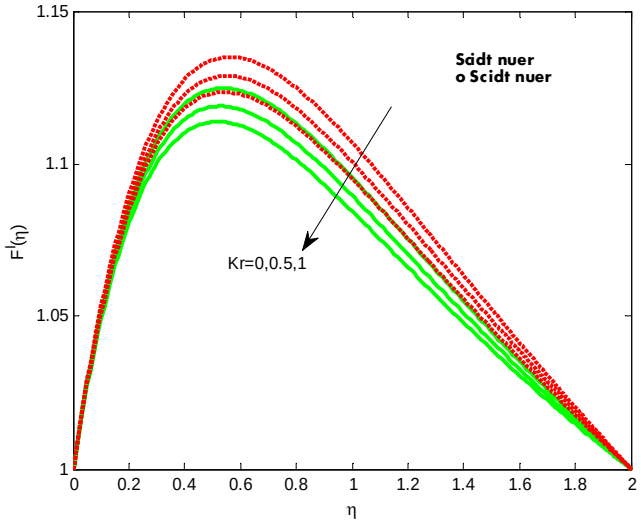

Figure 12. Velocity profiles for different values of chemical reaction parameter

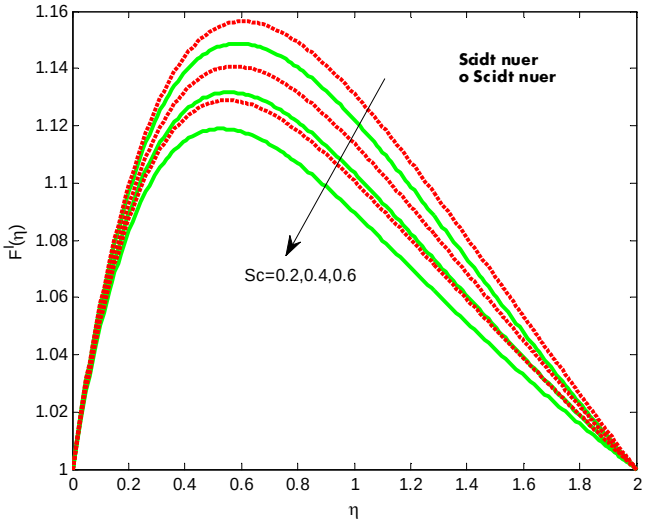

Figure 15. Velocity profiles for different values of Schmidt number

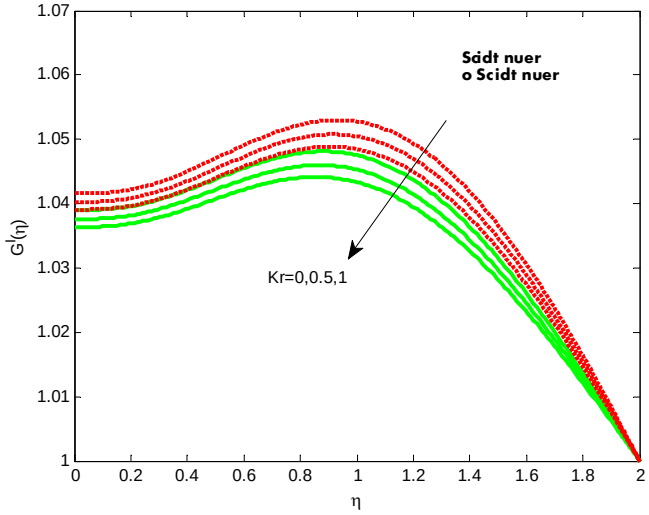

Figure 13. Induced magneticfield profiles for different values of chemical reaction parameter

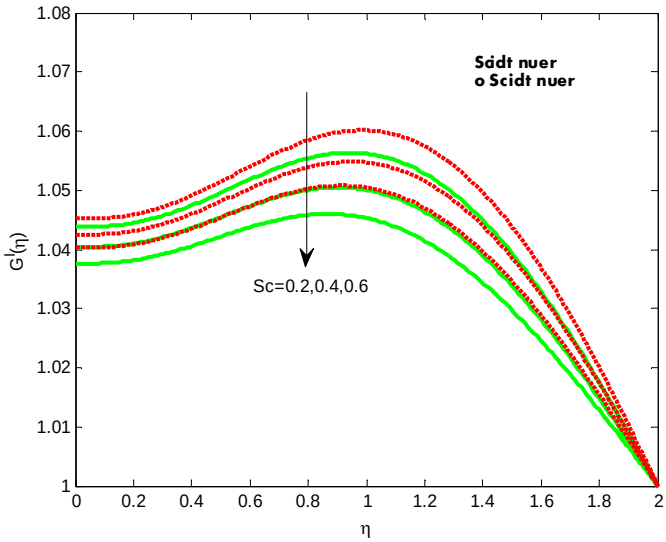

Figure 16. Induced magneticfield profiles for different values of Schmidt number

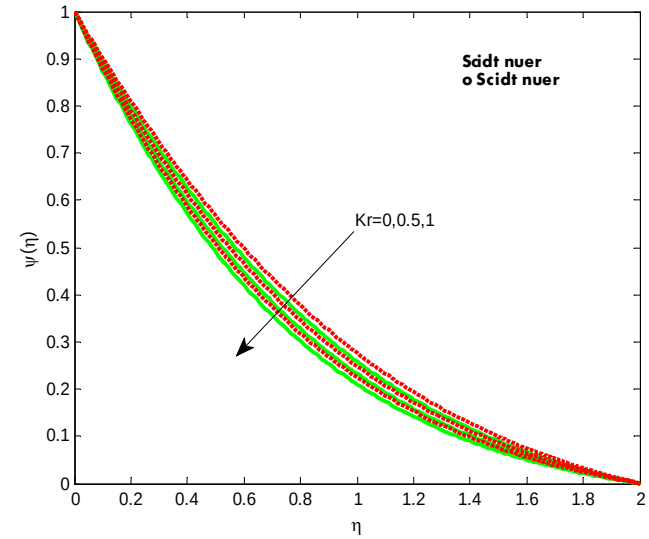

Figure 14. Concentration profiles for different values of chemical reaction parameter

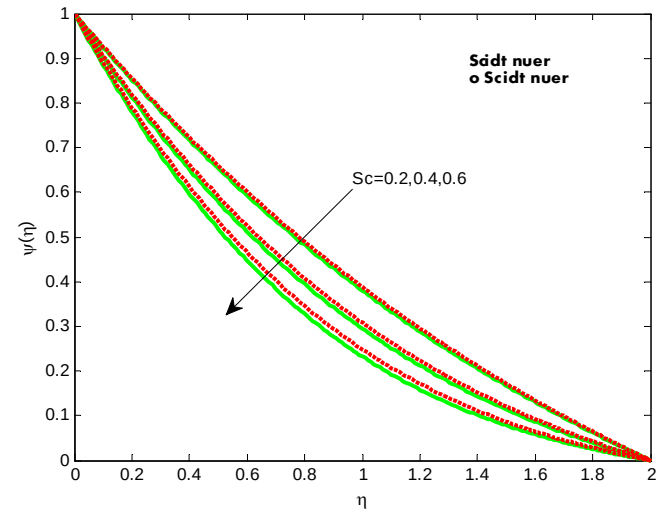

Figure 17. Concentration profiles for different values of Schmidt number

Table 2 Variation in $f''(0), -\theta'(0)\ and\ -\phi'(0)$ for injection case.

M	Kr	R	Q_H	Λ	Sc	$f''(0)$	$-\theta'(0)$	$-\phi'(0)$
0.2						0.565642	2.737094	1.128951
0.4						0.576611	2.738648	1.129931
0.6						0.587795	2.740232	1.130933
	0					0.625680	2.745754	1.009166
	0.5					0.610677	2.743472	1.132994
	1.0					0.597440	2.741463	1.247539
		0.2				0.590791	3.102580	1.131608
		0.4				0.604493	2.848369	1.132553
		0.6				0.616490	2.649800	1.133415
			0			0.626259	2.390493	1.134026
			0.5			0.610677	2.743472	1.132994
			1.0			0.597986	3.062155	1.132174
				0		0.390218	2.723303	1.124160
				0.5		0.500950	2.733496	1.128624
				1.0		0.610677	2.743472	1.132994
					0.2	0.672249	2.753061	0.751547
					0.4	0.637791	2.747690	0.957567
					0.6	0.610677	2.743472	1.132994

IV. CONLUSIONS

This study presents a numerical solution for the buoyancy-driven MHD mixed convection stagnation-point flow, heat and mass transfer of a nanofluid over a non-isothermal stretching sheet in presence of induced magneticfield, radiation, chemical reaction, suction/injection and heat source/sink. Conclusions of the present study are made as follows:

- Dual solutions exist only for certain range of suction/injection parameter.
- Chemical reaction parameter have tendency to improve mass transfer rate and depreciate the friction factor along with heat transfer rate.
- A raise in the value of magneticfield parameter enhances the heat and mass transfer rate.
- An increase in buoyancy parameter enhances the induced magneticfield profiles.
- A raise in the value of Schmidt number declines the momentum and thermal boundary layers.

ACKNOWLEDGMENT

Authors acknowledge the UGC for financial support under the UGC Dr. D. S. Kothari Post-Doctoral Fellowship Scheme (No.F.4-2/2006 (BSR)/MA/13-14/0026).

REFERENCES

Abdul Hakeem, A.K., Kalaivanan, R., Vishnu Ganesh, N., Ganga, B.2014. Effect of partial slip on hydro magnetic flow over a porous stretching sheet with non-uniform heat source/sink, thermal radiation and wall mass transfer, Ain Shams Engineering Journal. 5(3): 913-922.

Akbar, N.S., Raza, M., Ellahi, R. 2015. Influence of induced magneticfield and heat flux with the suspension of carbon nanotubes for peristaltic flow in a permeable channel. J. Magnetism and Mag Materials. 381:405-415.

Ali, F.M., Nazar, R., Arifin, N.M., Pop, I. 2011. MHD stagnation point flow and heat transfer towards stretching sheet with induced magnetic field. Appl Math Mech Engl Ed. 32(4):409–418.

Bhattacharya, K. 2013. Boundary layer stagnation point flow of Casson fluid and heat transfer towards a Shrinking/ Stretching sheet. Frontiers Heat Mass Transfer 4: Article ID: 023003.

Chandra Mandal, I., Swati, M. 2013. Heat transfer analysis for fluid flow over an exponentially stretching porous sheet with surface heat flux in porous medium. Ain Shams eng. Journal. 4:103-110. http://dx.doi.org/10.1016/j.asej.2012.06.004.

Cortell, R. 2014. MHD (magneto-hydrodynamic) flow and radiative nonlinear heat transfer of a viscoelastic fluid over a stretching sheet with heat generation/absorption. Energy. 74:896- 905.

Elbashbeshy, E.M.A. 2001. Heat Transfer over an exponentially stretching continuous surface with suction. Archives of Mechanics 53(6):643-651.

Hayat, T., Asad, S., Mustafa, M., Alsaedi, A. 2014. Radiation effects on the flow of Powell- Eyring fluid past an unsteady inclined stretching sheet with non-uniform heat source/sink. Plos one 9(7): e103214. doi:10.1371/journal.pone.0103214.

Jayachandra Babu, M., Radha Gupta, Sandeep, N. 2015. Effect of radiation and viscous dissipation on stagnation-point flow of a micropolar fluid over a nonlinearly stretching surface with suction/injection. Journal of Basic and Applied Research International 7(2):73-82.

Makinde, O.D., Aziz, A. 2011. Boundary layer flow of a nanofluid past a stretching sheet with convective boundary condition. Int. J. Therm. Sci., 50: 1326–1332.

Makinde, O.D., Khan, W.A., Khan, Z.H. 2013. Buoyancy effects on MHD stagnation point flow and heat transfer of a Nanofluid past a convectively heated stretching/shrinking sheet, Int.J.Heat and Mass transfer. 62:526-533.

Massoudi, M., Ramezan, M. 1990. Boundary layer heat transfer analysis of a viscoelastic fluid at a stagnation point. ASME J Heat Transf. 130:81-86.

Mohankrishna, P., Sugunamma, V., Sandeep, N. 2014. Radiation and magneticfield effects on unsteady natural convection flow of a nanofluid past an infinite vertical plate with heat source, Chemical and Process Engineering Research. 25:39-52.

Mustafaa, M., Hayat, T., Obaidat, S. 2013. Boundary layer flow of a nanofluid over an exponentially stretching sheet with convective boundary conditions. Int.J.Numeric. Meth. for Heat &Fluid flow 23(6): 945-959.

Najib, N., Bachok, N., Arifin, M.D., Ishak, A. 2014. Stagnation point flow and mass transfer with chemical reaction past a stretching/shrinking cylinder. Scientific Reports 4:4178, DOI: 10.1038/srep04178 (2014).

Pal, D., Mandal, G. 2014. Influence of thermal radiation on mixed convection heat and mass transfer stagnation-point flow in nanofluids over stretching/shrinking sheet in a porous medium with chemical reaction. Nuclear Eng and Design. 273:644-652.

Raju, C.S.K, Sandeep, N, Sulochana, C., Sugunamma, V., Jayachandrababu, M. 2015. Radiation, inclined magnetic field and cross-diffusion effects on flow over a stretching surface. Journal of the Nigerian Mathematical Society, 34:169-180.

Raju, C.S.K, Sandeep, N, Sulochana, C., Sugunamma, V. 2015. Effects of aligned magneticfield and radiation on the flow of ferrofluids over a flat plate with non-uniform heat source/sink. Internat. J. Sci. Eng., Vol. 8(2):151-158.

Rana, P., Bhargava, R. 2012. Flow and heat transfer of a nanofluid over a nonlinearly stretching sheet: a numerical study. Commun. Nonlinaer Sci.Numer.Simulation. 17:212-226.

Rashidi, M.M., Rostami, B., Freidoonimehr N., Abbasbandy, S. 2014. Free convective heat and mass transfer for MHD fluid flow over a permeable vertical stretching sheet in the presence of radiation and buoyancy effects. A S Engineering Journal 5:901-912.

Rohni, A.M., Ahmad, S., Pop, I. 2014. Flow and heat transfer at a stagnation point over an exponentially shrinking vertical sheet with suction. Int.J.Thermal Sciences 75:164-170.

Sandeep, N., Reddy, A.V.B., Sugunamma, V. 2012. Effect of radiation and chemical reaction on transient MHD free convective flow over a vertical plate through porous media.
Chemical and process engineering research. 2:1-9.

Sandeep, N., Sulochana, C. 2015. Dual solutions of radiative MHD nanofluid flow over an exponentially stretching sheet with heat generation or absorption. App. Nano. Science 5: (In Press)
DOI 10.1007/s13204-015-0420-z.

Sandeep, N., Sugunamma, V., Mohankrishna, P. 2013. Effects of radiation on an unsteady natural convective flow of a EG-Nimonic 80a nanofluid past an infinite vertical plate. Advances in Physics Theories and Applications, 23:36-43.

Sheikholeslami, M., Ganji, D.D., YounusJaved, M., Ellahi, R. 2015. Effect of thermal radiation on magnetohydrodynamic Nanofluid flow and heat transfer by means of two phase model. Journal of Magnetism and Magnetic Materials 374:36-43.

Subhashini, S.V., Sumathi, R., Momoniat, E. 2014. Dual solutions of a mixed convection flow near the stagnation point region over an exponentially stretching/shrinking sheet in nanofluids. Meccanica 49(10): 2467-2478.

Sulochana, C., Sandeep, N. 2015. Stagnation-point flow and heat transfer behavior of Cu-water nanofluid towards horizontal and exponentially stretching/shrinking cylinders, Applied Nanoscience 5: (In Press)